Experimental Study on Spring Constants of Structural Glass Panel Joints Under In-Plane Loading

Saddam Hussain*, Pei Shan Chen, Nagisa Koizumi, Baoxin Liu and Xiangdong Yan

Department of Civil Engineering and Architecture, Kyushu Institute of Technology, Kitakyushu 804-0015, Japan

ABSTRACT

Commonly, the columns and beams of glass panels are frequently subjected to in-plane loading, in which their joints will transfer the in-plane forces. Therefore, it is necessary to investigate the spring constants of the joints of these glass panels for the mechanical analysis of the structures. However, few issues were published on this subject, so estimating the spring constants of glass structure joints is important. Devote themselves to proposing methods to evaluate the spring constants of the joints of structural glass panels. This study tests two types of glass panels with thicknesses of 12 mm and 19 mm based on static and cycling loading. In addition, two types of Cushions: (1) aluminum and (2) rubber with a hardness of 65 and 90 degrees, are set between steel bolt(s) and glass panel(s) for the experiments. The spring constants are determined by the ratios of measured loads and the displacements between the glass panels and bolts. In addition, the authors proposed an equation to evaluate the bending spring constant from its axial spring constant determined by the loading tests. The experimental results showed that the joints with the aluminum cushion appear exactly non-linear elasticity while loading and unloading. Also, the pin junction within the central region (no Curve) is 0.6 mm. It is also determined that aluminum (cushion) slides of approximately ±0.3 mm under compression and tension. While loading (Tension/compression) is incremental, rubber acts nonlinearly but linear as unloaded.

E-mail addresses:
saddam.hussain372@mail.kyutech.jp (Saddam Hussain)
chen.pei-shan156@mail.kyutech.jp (Pei Shan Chen)
koizumi.nagisa830@mail.kyutech.jp (Nagisa Koizumi)
Liu.baoxin510@mail.kyutech.jp (Baoxin Liu)
yan.xiangdong760@mail.kyutech.jp (Xiangdong Yan)
* Corresponding author

INTRODUCTION

The authors are researching to realize frameless glass structures as new structural art. The frameless glass structure is close to pure glass, composed of tempered glass panels and minimal metal joints, expanding

the possibilities of unique architectural designs with excellent lighting (Santarieso et al., 2019; Centelles et al., 2019). However, the mechanical analysis and/or structural calculation for the frameless glass structures need the spring constants of its joints subjective to in-plane forces, as mentioned below. However, evaluating the spring constants of structural glass joints remains an unsolved issue. Therefore, the paper reports some important experimental results and methodology to evaluate the spring constant.

Researchers proposed some new structural systems to realize frameless glass structures as a kind of new structural system (Hussain et al., 2021; Bedon et al., 2019; Bedon et al., 2018a; 2019b). The frameless glass structure system comprises tempered glass panels and small metal joints, expanding the possibilities for unique architectural designs (Dispersyn et al., 2016; Chen, 2008). Inspired by the configuration of 1.5-Layer Space Frames, several assembling patterns for frameless glass are proposed by Chen (2011), and Figure 1 shows two examples of the proposals.
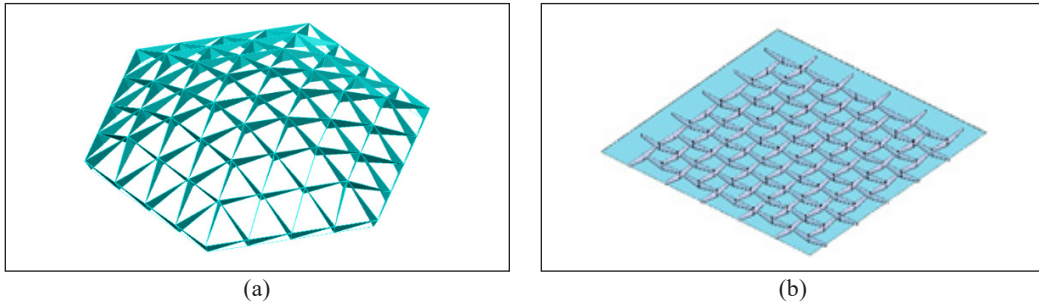

| (a) | (b) |

Figure 1. Examples of frameless glass structures: (a) Reciprocal Triple-Connecting glass structure; and (b) Lap panel frameless glass structure

For a frameless glass structure, the joints are important key parts. In earlier research by Chen (2010), some examples of three-dimensional connections are proposed. Figure 2(a) shows a common example of connecting two glass panels with aluminum sheets and bolts. Another example of the Lap assembling method is shown in Figure 2(b), in which the joints are designed to transfer the forces.
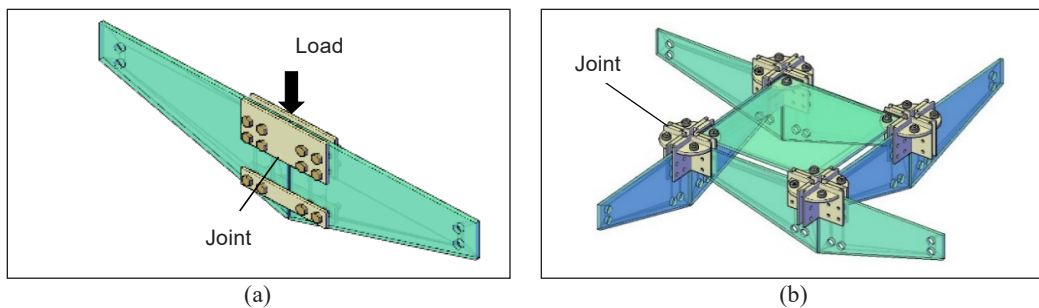

| (a) | (b) |

Figure 2. The analytical models of joints: (a) One-piece glass panel; and (b) Lap-unit

In common, the Finite element method (FEM) can analyze a glass panel by meshing it into many elements, as in the meshed glass panel shown in Figure 3. However, it is difficult to analyze the whole structure with FEM because all the glass panels consisting in the structure have to mesh and analyzed (Hadimam et al., 2008; Overed et al., 2007; Hussain et al., 2022; Honfi et al., 2014), which may cost more Central Processing Unit (CPU) time. Accordingly, a methodology for structural design and mechanical analysis for the whole structure is proposed, which transforms the glass panels into equivalent beams of the same bending stiffness and axial stiffness (Chen & Tsai, 2019; Giaralis & Spanos, 2010). As shown in Figure 3, the glass panels are replaced by beams, and joints are transformed into springs in axial and rotating directions for mechanical analyses of the whole structure. Therefore, the investigation of the spring constant for joints is required.
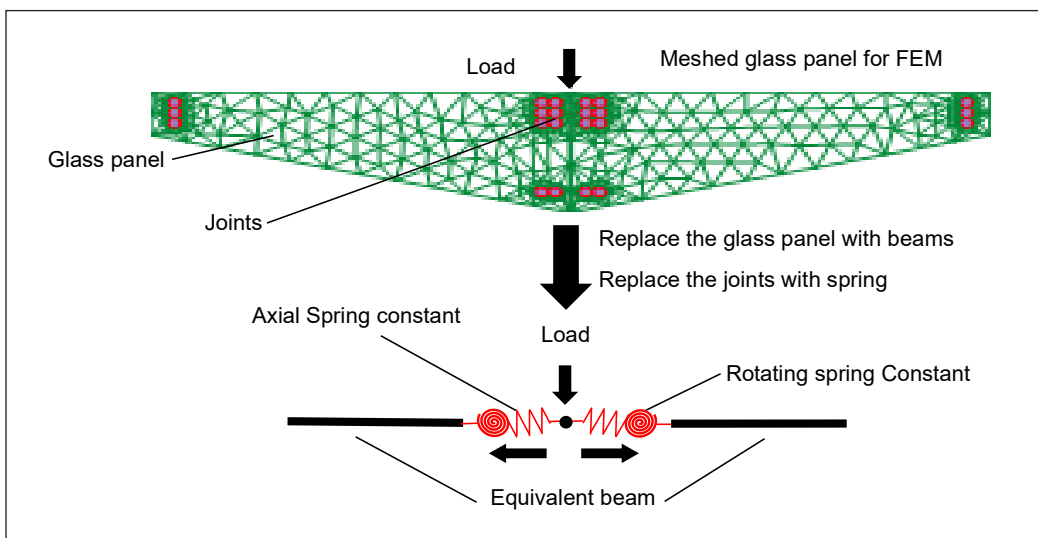

Figure 3. Replacing a glass panel with an equivalent beam method

However, few or no previous issues focused on the spring constants of the joints connecting glass panels. Accordingly, due to the lack of experimental research on such a topic, it appears vital to investigate the mechanical properties and develop a methodology to calculate the spring constants of joints of the structural glass panels. The design method of the three-dimensional combined glass panel structure proposed in the previous research, structural analysis, was proposed by the substitution method, as shown in Figure 3. When replacing the glass panel with an equivalent beam, the structure with a cylindrical curved surface cannot generate axial force in the glass surface. Therefore, here authors propose a structural design method in which a glass panel is used as an equivalent beam, and the joint portion is replaced with a spring. Therefore, a spring constant for the junction portion is required, and it is necessary to obtain this by experiment.

The final objective of this research is to complete the structural design theory of frameless glass structures and to put it into practical use. This paper evaluates the mechanical properties of glass joints, which are essential for structural analysis and calculation, especially their spring constants. The spring constants of tempered glass plate joints are experimental. The purpose of this research is to propose methods for calculating the spring constants of the joints for the structural glass panel. Based on the experimental results, the authors propose an equation to evaluate the bending spring constant for the mechanical analysis of the frameless glass structures.

MATERIALS AND METHODS

Mechanical Principle

In common, the seismic and/or wind loads could be considered recycling loading acting on the members and the joints connecting the structural members. Therefore, the authors experiment with recycling loading (compression/tension) to investigate the spring constant of the joints. This study uses an experimental setup to measure the displacements between the joint bolts and the glass panels with the recycling load. In subsequence, the spring constant can be calculated as the load-displacement ratio.

Experimental Setup

The experimental setup frame shown in Figure 4 is used for compression-tension tests to measure the displacements between the glass panels and the bolts. Notably, the load is applied with a double-action jack, and the load cell connected to the jack is used to measure the compression and tension load.
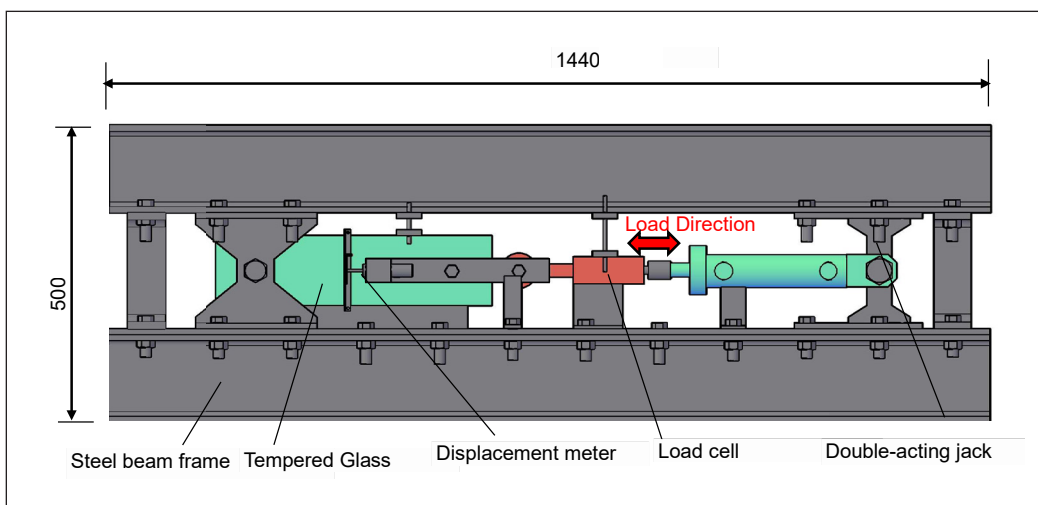

Figure 4. Assembly of the experimental setup (dimensions in mm)

Figure 5 exhibits that between the bolts and holes, there is a cushion. The bolt (a) is used to fix the glass panel to the experimental setup frame. The load is transferred through bolt (d) from the load cell connecting to the jack. The displacement meters are connected to the aluminum bars on both sides, which are used to measure the displacement between the stoppers and bolts (b)-(c); the stoppers are connected to the glass panel surface.
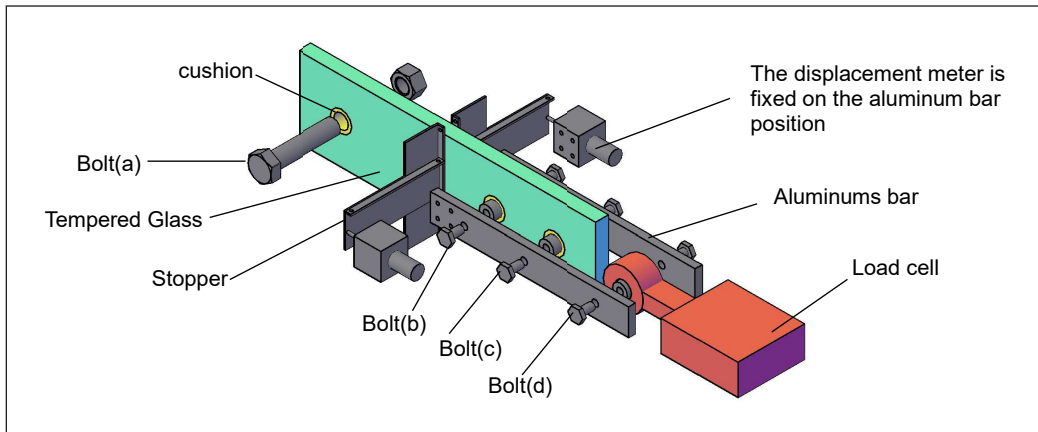

Figure 5. Details of specimen position during loading

As illustrated in Figure 6, two cushion materials are used,1) chloroprene rubber (CR), a couple of hardness (Hs) types (90, 65), labeled as CR Hs90 and CR Hs65, respectively, and 2) aluminum A5052 Japanese Industrial Standards (JIS) labeled as A5052.

Consequently, these cushion materials prevent direct contact between the bolt and the glass. The bolt-hole diameter is 32 mm, and the thickness of the cushion material is 5 mm. Bolts of M22 (S45C material, JIS) are utilized.

The Specimens

The specimens are two types of tempered glass panels with 19 mm and 12 mm thicknesses, respectively. Moreover, two types of joints with two holes and one hole are used, as shown in Figure 7. The panels are 450 mm and 120 mm long and wide, respectively. In addition,

Figure 6. Cushion material and dimensions: (a) Diameter of cushioning; and (b) Cushion material (dimensions in mm)

spacing of 90 mm bolt-to-bolt and 65 mm between the edges of the glass panel and bolt hole is provided. Further details of the specimens are presented in Table 1.
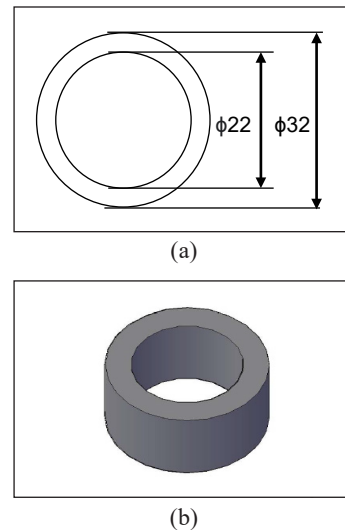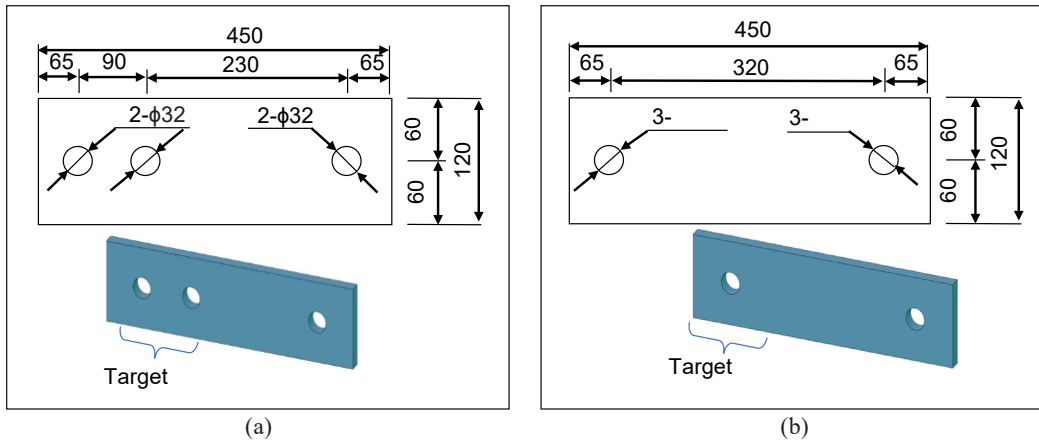
Figure 7. Specimen type and dimension: (a) Specimen with two holes; and (b) Specimen with one hole (dimensions in mm)

Table 1
Details of experimental specimens

Specimen type	Symbols		
	Cushion CR Hs90	Cushion CR Hs65	Cushion A5052
19mm-2	19-2-CR Hs90,	19-2-CR Hs65	19-2-A5052
19mm-1	19-1-CR Hs90	19-1-CR Hs65	19-1-A5052
12mm-2	12-2-CR Hs90	12-2-CR Hs65	12-2-A5052
12mm-1	12-1-CR Hs90	12-1-CR Hs65	12-1-A5052

The Recycle Loading

For the joints with rubber Cushions (90,65) degrees, the peak load is ±3600N, and ten times recycling loading is performed for the experiments. At the same time, each time incremental of repeating load is set as a ±400N. For the joints with aluminum cushion, ten times of recycling loading are performed for tests, and the peak load for each repeating is set as ±5000N, ±7000N, ±10000N, and ±15000N.

RESULTS AND DISCUSSION

Summary of the Experimental Results

Experimental testing of glass panels is illustrated in Figure 8. The load-displacement curves are shown in Figures 9 to 12. The displacement measured in the experiments is the average of the two displacement meters set on both sites of the glass panel.

Figure 9(a) shows the results of specimens 19-2-CR Hs90, and the maximum applied load is ±3600N. The maximum and minimum displacements are 2.409 mm and -3.149 mm, respectively. Figure 9(b) shows the outcomes of 19-2-CR Hs65. It is indicated that the maximum and minimum displacements are 3.487mm and -3.806 mm, respectively.

The average displacement is 0.159 mm. In Figure 9(c), the outcome of 19-2-A5052, the maximum applied load is ±15000N; consequently, the maximum displacement is 0.456 mm, and the minimum displacement is -0.576 mm. Moreover, the load does not enhance up to a displacement of ±0.3 mm, and bolts and glass panels slide with each other.

Figure 10(a) presents the result of 19-1-CR Hs90, in which the maximum load implicates to ±3600N. As a result, the maximum and minimum displacement is found to be 3.804 mm and - 4.149 mm, respectively. The average of the peak displacements is 3.999 mm. Figure 10(b) expresses the load-displacement curves for 19-1-CR Hs65, where the maximum load is ±3600N. The maximum and minimum displacements were 3.958 mm and -3.918 mm, respectively. It is illustrated in Figure 10(c) for 19-1-A5052, and it is observed that the maximum load is ±7000N, and the maximum displacement was 0.975

Figure 8. Experimental setup and specimens during the performing test
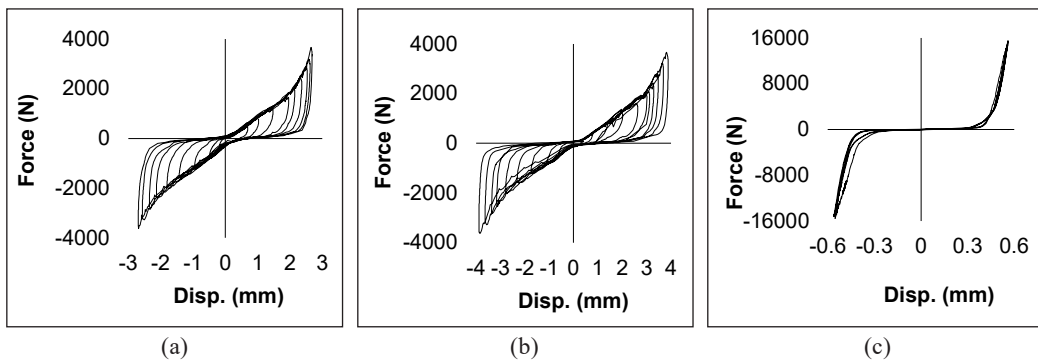

| (a) | (b) | (c) |

Figure 9. Recycling loading of test of 19mm thickness glass panel with 2 bolt holes: (a) 19-2-CR Hs90; (b) 19-2-CR Hs65; and (c) 19-20A5052
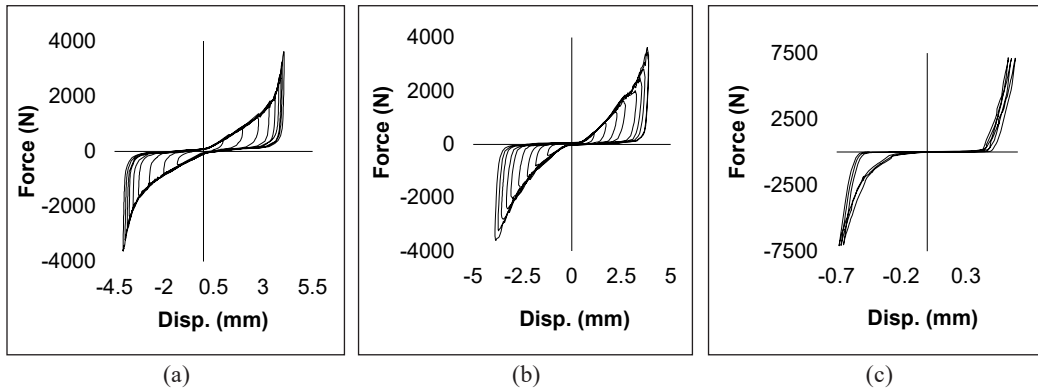
Figure 10. Recycling loading of test of 19mm thickness glass panel with 1 bolt hole: (a) 19-1-CR Hs90: (b) 19-1-CR Hs65; and (c) 19-1-A5052

mm; the minimum displacement was -0.388 mm. Furthermore, the average displacement is ±0.2935 mm.

Figure 11(a) indicates the result of 12-2-CR Hs90 with a maximum load of ±3600N, 3.884 mm is the maximum displacement, and minimum displacement is determined as -3.662 mm, which the average displacement is ±0.111 mm. Figure 11(b) presents the displacement results for 12-2-CR-Hs65. The maximum and minimum displacements were 3.395mm and -3.707 mm, respectively. The maximum load is 3600 N, and the average displacement is ±0.156 mm. Figure 11(c) indicates the outcome of 12-2-A5052; the max load is ±10000N. As a result, the maximum displacement is 0.495 mm, the minimum displacement is -0.746 mm and the average displacement is ±0.6205 mm.

Figure 12(a) depicts the result of 12-1-CR Hs90 on a maximum load of ±3600N, and the average displacement is 4.093 mm. Figure 12(b) shows the outcomes of 12-1-CR Hs65 with the maximum load of ±3600N. The maximum displacement is 4.560 mm, the minimum is 3.315 mm, and the average is 3.938 mm. Figure 12(c) shows the result of 12-1-A5052 with a maximum load of 5000N. The maximum and minimum displacements are 0.785 mm and 0.283 mm, respectively. Moreover, the average displacement is ±0.251 mm.
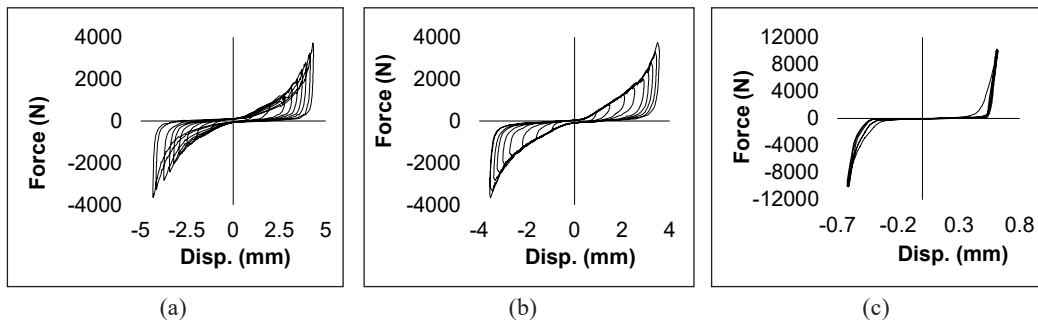

Figure 11. Recycling loading of 12mm thickness glass panel test with 2 bolt holes: (a) 12-2-CR Hs90: (b) 12-2-CR Hs65; and (c) 12-2-A5052
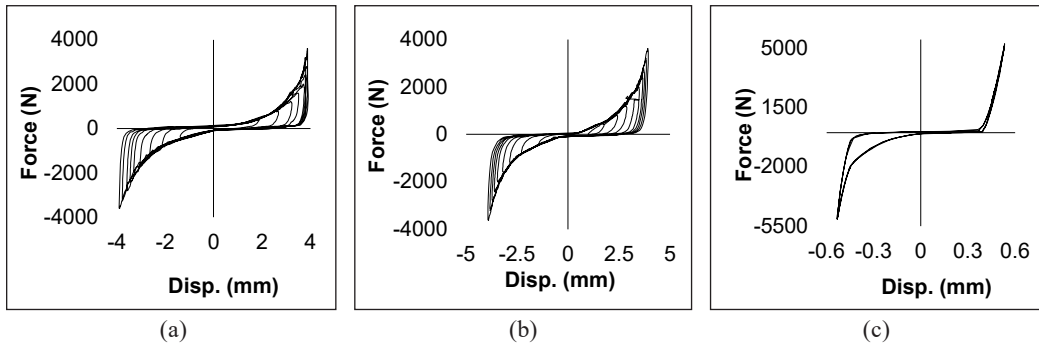
Figure 12. Recycling loading of test of 12mm thickness glass panel and 1 bolt hole: (a) 12-1-CR Hs90: (b) 12-1-CR Hs65; and (c) 12-1-A5052

Estimation of the Spring Constants

In the frameless glass structure, axial forces are applied in the tempered glass panels. As mentioned, the authors proposed replacing the tempered glass panels with equivalent beams and the joints with springs for the mechanical analysis with a model consisting of all structural members. The spring constants can be obtained from the load-displacement ratio, in which the displacement is measured between the glass panel and bolts under in-plane loading.

Figure 13(a) presents the recycling curve of the specimens with a rubber cushion, which is close to a straight line during increasing loading and shows a non-linear curve during unloading. Figure 13(b) shows the load and displacement curve of the specimens with the aluminum cushion, which shows non-linear elasticity while loading and unloading. Furthermore, the curve appears as a pin junction within the central region, as shown in the diagram. It is also determined that aluminum (cushion) slides of approximately ±0.3 mm under compression and tension.
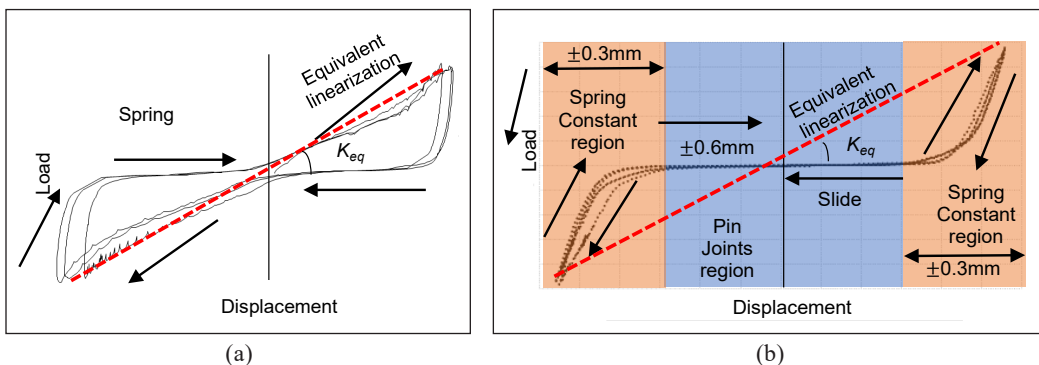

Figure 13. Mechanical behavior of the spring constants joint: (a) Chloroprene rubber cushioning material; and (b) Aluminum cushioning material

The proposed mechanical analysis methodology, especially for dynamic mechanical analysis during seismic design, is based on equivalent linearization. The equivalent linearization replaces each non-linear stiffness with a quasilinear stiffness (Koliopulos et al., 1994; Overend, 2007). It inspires authors to find the spring constant for the mechanical analysis with equivalent linearization. The spring constant of equivalent linearization is directly proportional to the average forces (P_{max} and P_{min}) and the associated values of the average displacements (δ_{max} and δ_{min}). Figure 13 shows the image of spring constants of equivalent linearization with the slope of red lines, which connects the peak points of forces and displacements. The spring constant of equivalent linearization K_{eq} is calculated in Table 2.

Table 2
Spring constants for equivalent linearization (unit: N/mm)

Spring constants, K_{eq}	CR Hs90	CR Hs65	A5052
19mm-2	1248.60	942.65	27363.73
19mm-1	863.72	863.56	1040.5
12mm-2	911.37	955.33	16120.06
12mm-1	829.02	850.44	9641.47

Calculation Formula of Spring Constant for Bending

This discussion elaborates an equation to calculate the bending spring constant K_R from its axial spring constant K_A determined by the loading tests. Figure 14 exhibits the calculation model; a and l indicate the distances between the bolts, C_1, C_2 and T describe the forces acting on the bolts, and δ_1, δ_2, and δ_3 in Equation 1 represent the displacements between the bolts and glass panel.

In this calculation and derivation model shown in Appendix A, the distance from the top bolt center to the neutral axis is x_n, which the following calculation can derive. $x_n = \frac{a+l}{3}$,
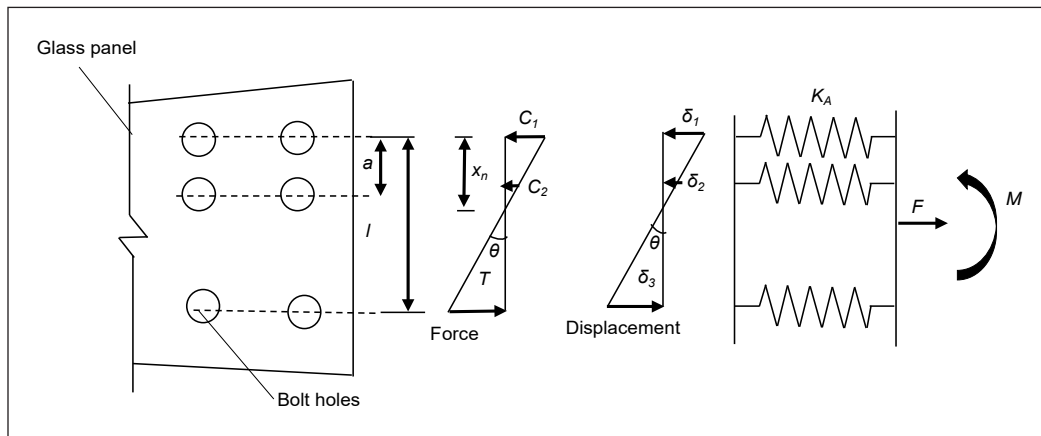

Figure 14. Calculation model for constant spring calculation

Consequently, the moment can be expressed by the distance between the neutral axis and bolts, which can be modified using Equation 2 in Appendix A.

$$M = \frac{x_n{}^2 + (x_n\text{-}a)^2 + (l\text{-}x_n)^2}{x_n} \cdot \delta_1 \cdot K_A \tag{1}$$

The bending spring constant(K_R)is defined as $K_R = \dfrac{M}{\theta}$, where the bending angle θ can be calculated by Equation 3.

$$\theta = \frac{\delta_1 + \delta_3}{l} = \left(\delta_1 + \frac{l\text{-}x_n}{x_n} \cdot \delta_1 \right) \cdot \frac{1}{l} = \frac{\delta_1}{x_n} \tag{2}$$

$$K_R = \frac{2}{3} \cdot \left(a^2 + l^2 - a \cdot l \right) \cdot K_A \tag{3}$$

CONCLUSION

In this study, the authors conducted experiments and theoretical research to evaluate the spring constants of structural glass panel joints. Moreover, the spring constant for equivalent linearization K_{eq} was summarized in 800-1000N/mm. It was found that the specimen with rubber cushion exhibited non-linear behavior. Specimens with aluminum cushions exhibit a slip of approximately ±0.3 mm and behavior elastic non-linear during compression and tension. It can be set as a pin joint in this region. The spring constant for equivalent linearization of specimens with aluminum cushions is summarized as 10000-27000N/mm. Future issues include a problem with the mechanism of this test specimen, which caused errors and a large amount of residual strain and slippage. The rubber may behave similarly and plasticize when the load is increased. It is considered feasible to propose a joint using aluminum or other materials. It is also necessary to study the spring constant by changing the approximation method based on the results of this experiment. Glass panel bolts from the market were investigated to limit the scope of the research. The bolts and their designs, including the, serve as the in-plane testing. The thickness of the glass is chosen based on experience, consultation, and avoiding too many sets of testing.

The future purpose of this study is to propose the structural design theory of the frameless glass structures, a three-dimensional combination glass panel structure. In addition, it determines the non-linear behavior elastic region behavior of spring constants in material joints and glass panels.

ACKNOWLEDGEMENTS

REFERENCES

Bedon, C., Amadio, C., & Noé, S. (2019). Safety issues in the seismic design of secondary frameless glass structures. *Safety*, *5*(4), Article 80. https://doi.org/10.3390/safety5040080

Bedon, C., & Santarsiero, M. (2018b). Transparency in structural glass systems via mechanical, adhesive, and laminated connections-existing research and developments. *Advanced Engineering Materials*, *20*(5), Article 1700815.

Bedon, C., & Santarsiero, M. (2018a). Laminated glass beams with thick embedded connections–Numerical analysis of full-scale specimens during cracking regime. *Composite Structures*, *195*, 308-324. https://doi.org/10.1016/j.compstruct.2018.04.083

Bedon, C., Zhang, X., Santos, F., Honfi, D., Kozłowski, M., Arrigoni, M., & Lange, D. (2018). Performance of structural glass facades under extreme loads - Design methods, existing research, current issues, and trends. *Construction and Building Materials*, *163*, 921-937.

Chen, P. S. (2008). A study report on an ancient chinese wooden bridge hongqiao, *Structural Engineering International, 18*(1), 84-87. https://doi.org/10.2749/1016866 08783726614

Chen, P. S. (2010, November 8-12). A study on the geometrical configuration of an ancient wooden bridge in *Qingming Shanghe Tu.* In *Proceeding of IASS2010.* Shanghai, China.

Chen, P. S. (2011, September 20-23). A report on the innovation of 1.5-layer space frames. In *Proceeding of IABSE IASS.* London, UK.

Chen, P. S., & Tsai, M. T. (2019). On configuration and structural design of frameless glass structures. In J. S. C. Paulo (Ed.), *Structures and Architecture: Bridging the Gap and Crossing Borders* (pp. 628-637). CRC Press. https://doi.org/10.1201/9781315229126

Centelles, X., Castro, J. R., & Cabeza, L. F. (2019): Experimental results of mechanical, adhesive, and laminated connections for laminated glass elements - A review. *Engineering Structures, 180*, 192-204. https://doi.org/10.1016/j.engstruct.2018.11.029

Dispersyn, J., & Belis, J (2016). Numerical research on stiff adhesive point-fixings between glass and metal under uniaxial load. *Glass Structures & Engineering, 1,* 115-130. https://doi.org/10.1007/s40940-016-0009-2

Giaralis, A., & Spanos, P. D. (2010). Effective linear damping and stiffness coefficients of nonlinear systems for design spectrum-based analysis. *Soil Dynamics and Earthquake Engineering*, *30*(9), 798-810. https://doi.org/10.1016/j.soildyn.2010.01.012

Hussain, S., & Chen, P. S. (2021). Future importance and demand of frameless glass structure. *World Journal of Advanced Scientific Research*, *4*(2), 1-19.

Honfi, D., Reith, A., Vigh, L. G., & Stocker, G. (2014). Why glass structures fail? Learning from failures of glass structures. In L. Christian, B. Freek, B. Jan & L. Jean-Paul (Eds.), *Challenging Glass 4 & Cost Action TU0905 Final Conference* (pp. 791-800). CRC Press. https://doi.org/10.1201/b16499

Hussain, S., Chen, P. S., Koizumi, N., Rufai, I., Rotimi, A., Malami, S. I., & Abba, S. I. (2022). Feasibility of computational intelligent techniques for the estimation of spring constant at joint of structural glass plates: a dome-shaped glass panel structure. *Glass Structures & Engineering, 8*, 141-157. https://doi.org/10.1007/s40940-022-00209-6

Koliopulos, P. K., Nichol, E. A., & Stefanou, G. D. (1994). Comparative performance of equivalent linearization techniques for inelastic seismic design. *Engineering Structures 16*(1), 5-10. https://doi.org/10.1016/0141-0296(94)90099-X

Santarsiero, M., Bedon, C., & Moupagitsoglou, K. (2019). Energy-based considerations for the seismic design of ductile and dissipative glass frames. *Soil Dynamics and Earthquake Engineering*, *125*, Article 105710. https://doi.org/10.1016/j.soildyn.2019.105710

Overend, M., De Gaetano, S., & Haldimann, M. 2007. Diagnostic Interpretation of Glass Failure. *Structural Engineering International*, *17*(2), 151-158. https://doi.org/10.2749/101686607780680790

APPENDIX A

In the session of results and discussions, Figure 14 demonstrates the calculation formula of spring constant for the bending model; a and l indicate the distances between the bolts, C_1, C_2, and T describe the forces acting on the bolts, and δ_1, δ_2, and δ_3 represents the displacements between the bolts and glass panel. The following Equation 4 indicates the basic conditions of force equilibrium.

$$T = C_1 + C_2 \quad ; \quad \delta_3 K_A = \delta_1 K_A + \delta_2 K_A \tag{4}$$

In this calculation model, the distance from the top bolt center to the neutral axis is x_n, Equation 5, which the following calculation can derive.

$$\frac{\delta_1}{x_n} = \frac{\delta_2}{x_n - a} = \frac{\delta_3}{l - x_n} \; ; \; \frac{l - x_n}{x_n} \cdot \delta_1 = \delta_1 + \frac{x_n - a}{x_n} \cdot \delta_1 \; ; \tag{5}$$

Consequently, the moment can be expressed by the distance between the neutral axis and the bolts as in Equation 6, which can be modified as Equation 7 using Equation 2.

$$M = x_n \cdot C_1 + (x_n - a) \cdot C_2 + (l - x_n) \cdot T \tag{6}$$

$$M = \frac{x_n^2 + (x_n - a)^2 + (l - x_n)^2}{x_n} \cdot \delta_1 K_A \tag{7}$$

The bending spring constant K_R is defined as Equation 8, where the bending angle θ can be calculated by Equation 7. Therefore, the bending rigidity spring constant K_R can be obtained by substituting Equations 8 and 9 into Equation 10.

$$K_R = \frac{M}{\theta} \tag{8}$$

$$\theta = \frac{\delta_1 + \delta_3}{l} = \left(\delta_1 + \frac{l - x_n}{x_n} \cdot \delta_1 \right) \cdot \frac{1}{l} = \frac{\delta_1}{x_n} \tag{9}$$

$$K_R = \frac{2}{3} \cdot (a^2 + l^2 - a \cdot l) \tag{10}$$